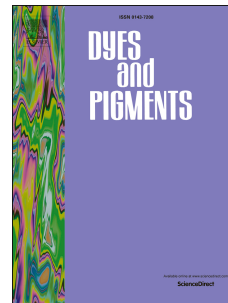


Accepted Manuscript

Rapid detection of aspartic acid and glutamic acid in water by BODIPY-Based fluorescent probe: Live-cell imaging and DFT studies

Subhajit Guria, Avijit Ghosh, Kalipada Manna, Abhishek Pal, Arghya Adhikary, Susanta Adhikari



PII: S0143-7208(19)30154-8

DOI: <https://doi.org/10.1016/j.dyepig.2019.04.052>

Reference: DYPI 7507

To appear in: *Dyes and Pigments*

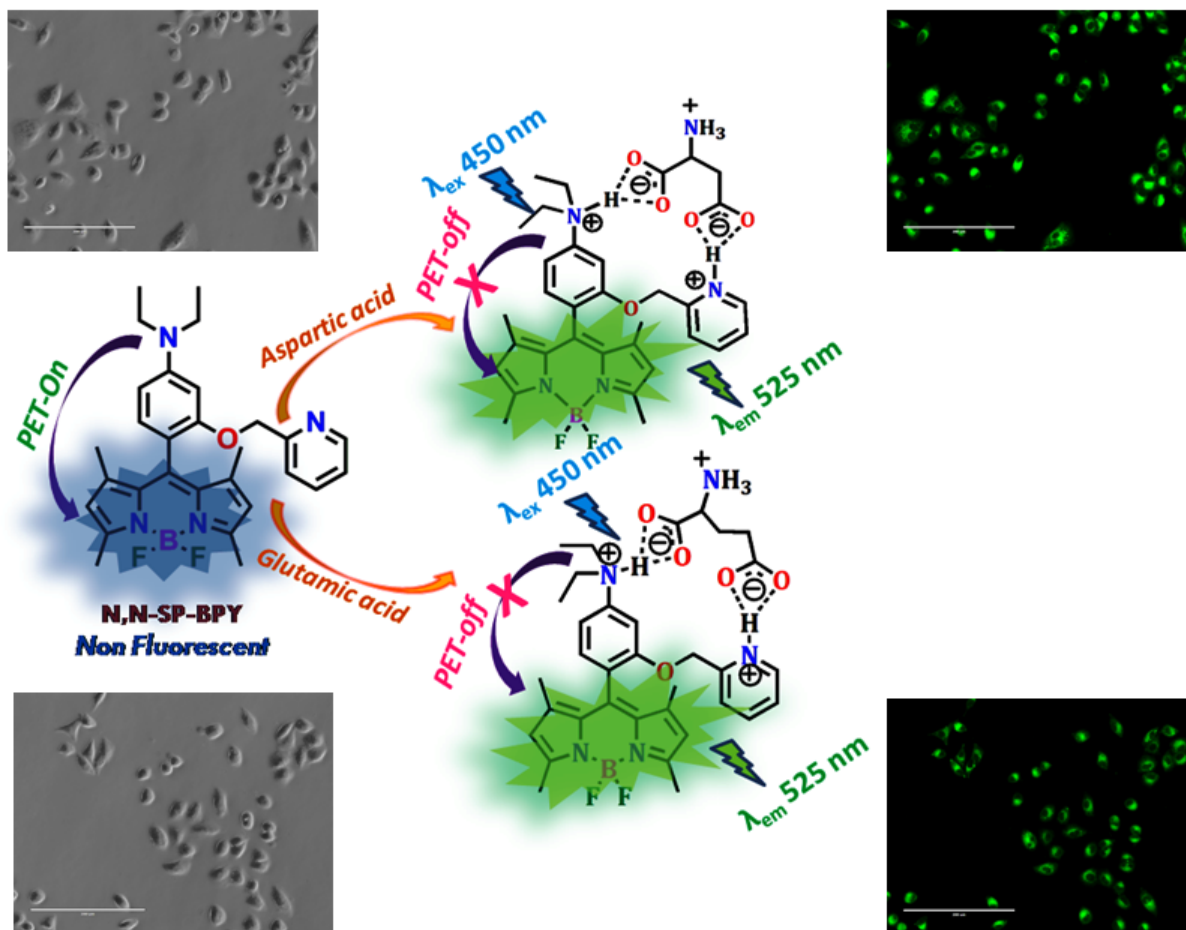
Received Date: 20 January 2019

Revised Date: 21 April 2019

Accepted Date: 22 April 2019

Please cite this article as: Guria S, Ghosh A, Manna K, Pal A, Adhikary A, Adhikari S, Rapid detection of aspartic acid and glutamic acid in water by BODIPY-Based fluorescent probe: Live-cell imaging and DFT studies, *Dyes and Pigments* (2019), doi: <https://doi.org/10.1016/j.dyepig.2019.04.052>.

This is a PDF file of an unedited manuscript that has been accepted for publication. As a service to our customers we are providing this early version of the manuscript. The manuscript will undergo copyediting, typesetting, and review of the resulting proof before it is published in its final form. Please note that during the production process errors may be discovered which could affect the content, and all legal disclaimers that apply to the journal pertain.



ACCEPTED

Rapid Detection of Aspartic acid and Glutamic acid in Water by BODIPY-Based fluorescent Probe: Live-Cell Imaging and DFT studies

Subhajit Guria,^[a] Avijit Ghosh,^[a,b] Kalipada Manna,^[a] Abhishek Pal,^[a] Arghya Adhikary,^[b] Susanta Adhikari,^{*[a]}

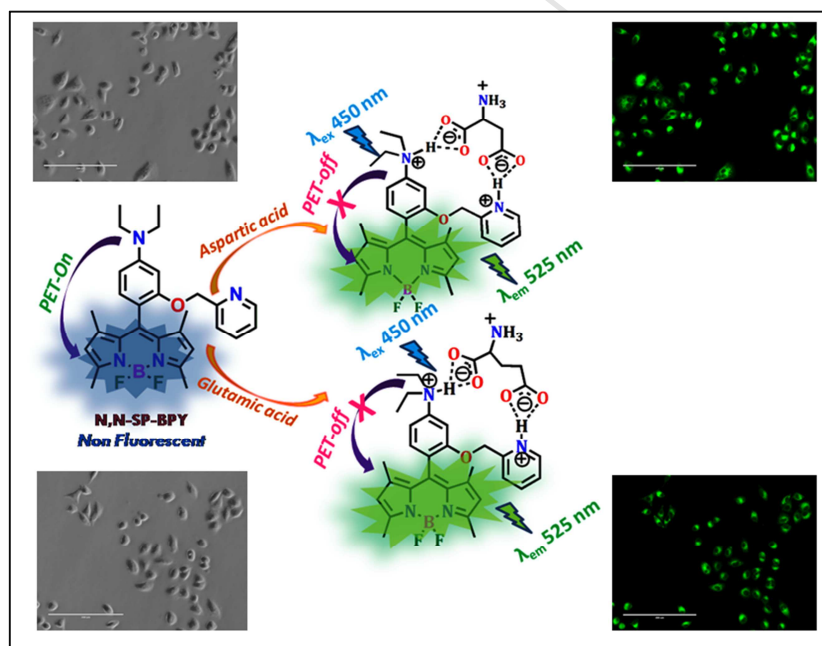
^aDepartment of Chemistry, University of Calcutta, 92, A.P.C. Road, Kolkata 700 009, West Bengal, India.

^bCentre for Research in Nanoscience & Nanotechnology, (CRNN), University of Calcutta, Technology Campus, Sector-III, Block-JD 2, Salt Lake, Kolkata 700098, West Bengal, India.

* To whom correspondence should be addressed.

E-mail address: adhikarisusanta@yahoo.com;

Graphical abstract



Highlights

1. A highly selective BODIPY probe, N,N-SP-BPY detects aspartic acid (Asp) and glutamic acid (Glu) in water.

2. 'Turn On' fluorescence can be observed by inhibition of Photoinduced Electron Transfer (PET) process.
3. A distinct colorimetric change from pink to colorless solution can be observed to recognize Asp and Glu.
4. N,N-SP-BPY efficiently images intracellular Asp and Glu in live cells under fluorescence microscope.

Abstract: Strategically modified 4-(diethylamino)-2-(pyridin-2-ylmethoxy)benzaldehyde appended BODIPY-based probe N,N-SP-BPY detects aspartic acid (Asp) and glutamic acid (Glu) by inhibition of Photoinduced electron transfer (PET) process in water. The probe shows considerable and rapid fluorescence enhancement upon addition of Asp and Glu. Additionally, a distinct colorimetric change from pink to a colorless solution can be observed to recognize traces of Asp and Glu. The probe detects Asp and Glu as low as 1 μM and 5 μM respectively. Furthermore, the probe can efficiently detect intracellular Asp and Glu in live HeLa, A549, MDA-MB-468 and HEK-293T cells under fluorescence microscope without showing any cytotoxic effect. Two model BODIPY derivatives are also synthesized to establish strategic modification. ^1H NMR titration and theoretical calculations strongly supports experimental findings.

Keywords: BODIPY • Photoinduced electron transfer process • Fluorescent probe • DFT calculation • Live cell imaging

1. Introduction

Aspartic acid (Asp) and glutamic acid (Glu) are dicarboxylic amino acids, and their conjugate base aspartate and glutamate, are a major excitatory neurotransmitter in the mammalian central nervous system (CNS). The concentration of aspartate in cerebrospinal fluid (CSF) is found to be 1.22 ± 0.21 mM, while the normal concentration of glutamate varies from few micromolar in the extracellular fluids to 1–10mM inside neurons of the brain [1-3].

Aspartic acid is a precursor for the synthesis of two other amino acids namely glutamic acid and glycine [4] and is recognized for its facilitating role in the tricarboxylic acid (TCA) cycle [5]. Researchers have also demonstrated the role of aspartic acid in hydroxyapatite [6] and osteoarthritis [7]. Excessive

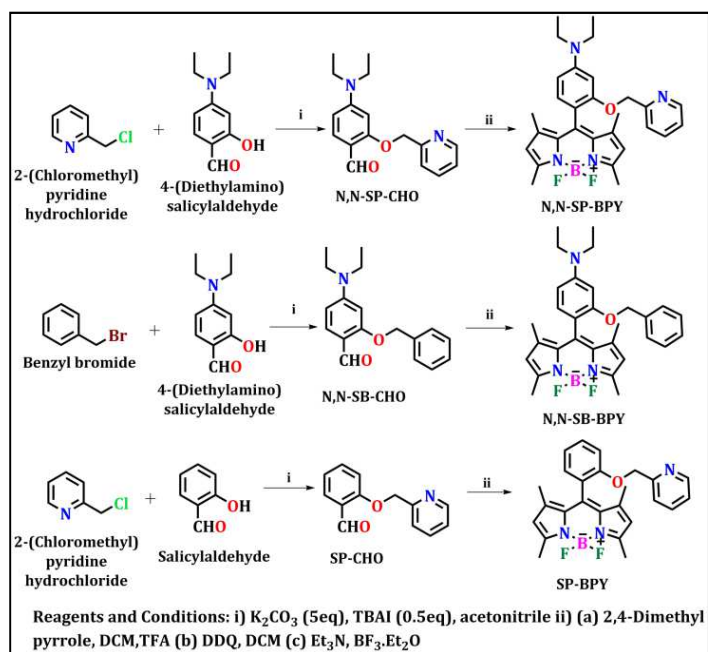
aspartic acid can be a reason for Lou Gehrig's disease [8] and is also associated with the early-onset dementia of the Alzheimer type [9].

Glutamic acid rich chain of bone sialoprotein, osteonectin and osteopontin are concerned in Hap nucleation and growth [10] as indicated by earlier research. It is also responsible for the biosynthesis of γ -aminobutyric acid (GABA) [11]. Glutamate is the prime mediator of sensory information, memory formation, memory retrieval, emotions and motor coordination [12]. In the food industry, its monosodium salt (MSG- monosodium glutamate) is a well-known flavour enhancer and generally found in different foods for achieving strong, balanced and preferred product flavour. However, accumulation of glutamate can be toxic to neurons and therefore, must be firmly regulated. The extreme intake of this flavour enhancer may cause allergic effects (headache and stomach pain) [13,14]. Patients with acute ischemic stroke have demonstrated high levels of glutamate in plasma and cerebrospinal fluid (CSF) [15]. In human and in animals, epileptic tissues have shown slow metabolic processing of glutamate and down-regulation of glutamate to glutamine cycle [16].

As these amino acids play a crucial role in many physiological pathways their biological monitoring is of utmost importance. Chromatographic techniques based on ion exchange,[17] GC (gas chromatography) [18], LC/MS approach [19], electrochemical [20-22] and infrared spectroscopy [23] are some of the popular analytical procedures for detection and characterization of amino acids. Molecules that can report the interaction of amino acids through changes in their optical properties (emission or absorption) i.e. chemosensors, could act as good candidates for the same [24-44]. Among the copious amount of highly fluorescent dyes that are available in the literature, sets based on 4,4-difluoro-4-bora-3a,4a-diaza-s-indacene1,2 (better known as BODIPY, Difluoroboron Dipyrromethene) shows the highest potential because of their robustness against light and chemicals. Their optical properties can also be easily tweaked by attachment of residues at the suitable position of the BODIPY core [45].

Herein, we report the synthesis of 4-(diethylamino)-2-(pyridin-2-ylmethoxy)benzaldehyde appended BODIPY based probe N,N-SP-BPY which detects Aspartic acid (Asp) and glutamic acid (Glu) by inhibition of Photoinduced electron transfer (PET) process in water. The probe N,N-SP-BPY shows strong fluorescent enhancement and a distinct change in naked eye colour of the solution from pink to colorless during the addition of Asp/Glu in water. The probe is also able to efficiently image Asp or Glu in live cells. The probe is weakly fluorescent due to the effective PET process operating from N,N-diethylamino unit of N,N-SP-BPY to BODIPY core. Inhibition of PET process occurs in the presence of Asp/Glu, leading to fluorescence enhancement. Two model compounds, N,N-SB-BPY, and SP-BPY were synthesized to comprehend the exact molecular mechanism associated with the changes that were taking place in fluorescence and UV-

Visprofile. Scheme 1 shows the synthetic procedure of the probe and model compounds. All the intermediates and probes were characterized by ^1H NMR, ^{13}C NMR and QTOF-MS (Figure S-1 to S-17, ESI). Theoretical calculations were performed to support the experimental observations.



Scheme-1: Synthetic route to **N,N-SP-BPY**, **N,N-SB-BPY** and **SP-BPY**

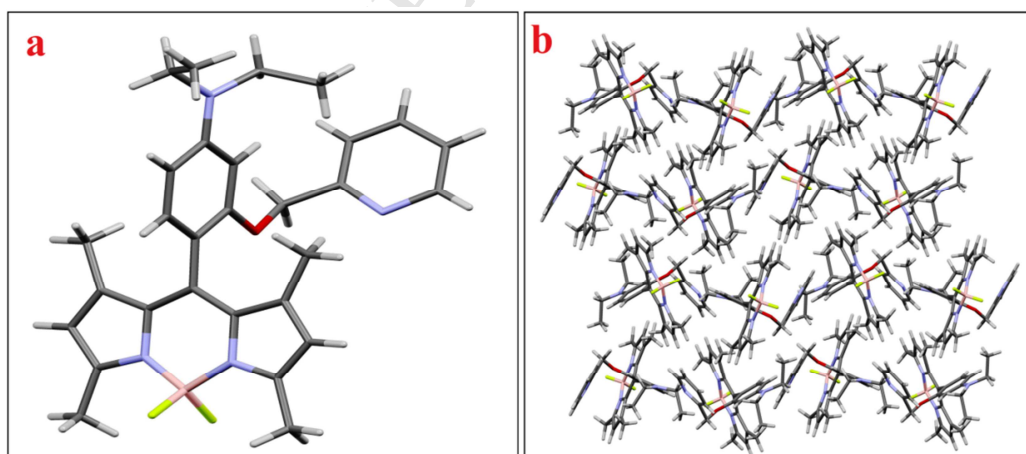


Figure 1: (a) Single crystal X-ray structure (CCDC 1902075), and (b) packing diagram of **N,N-SP-BPY**.

2. Experimental

2.1. Materials and Equipment:

Chemicals and solvents were purchased from commercial suppliers and used as received. ^1H and ^{13}C NMR spectra were recorded on a Bruker Advance III HD (300 MHz) spectrometer. Chemical shifts were reported in parts per million (ppm), and the residual solvent peak was used as an internal reference: proton (chloroform δ 7.26), carbon (chloroform δ 77.16) or tetramethylsilane (TMS δ 0.00) was used as a reference. Multiplicity was indicated as follows: s (singlet), d (doublet), t (triplet), q (quartet), m (multiplet). Coupling constants were reported in Hertz (Hz). High resolution mass spectra were obtained on a Xevo G2S/Q-ToF. microTM spectrometer. For thin layer chromatography (TLC), Merck precoated TLC plates (Merck 60 F254) were used and flash chromatography separations were performed on SRL 230-400 mesh silica gel.

2.2. In vitro cell imaging

Human cervical cancer HeLa, Breast cancer cell MDA-MB-468, Lung cancer cell A549, and normal HEK-293T cells were cultured in Dulbecco's modified eagle medium (DMEM) supplemented with 10% fetal bovine serum (FBS) and 1% penicillin/streptomycin at 37°C and 5% CO₂. For in vitro imaging studies, the cells were seeded in 12-well tissue culture plates with a seeding density of 10⁵ cells per well. After reaching 60%–70% confluence, the previous DMEM medium was replaced with serum-free DMEM medium (without any amino acid), supplemented with 20 μM N,N-SP-BPY and incubated for 2h to facilitate the probe uptake by cells. Then cells were washed three times with PBS buffer to remove any extracellular N,N-SP-BPY. Then Asp/Glu (50 μM) was added into the medium and then further incubated for 1 hour. After washing with PBS buffer, images of live cells were taken using an EVOS® FL Cell Imaging System, Life Technologies, USA).

2.3. Synthesis:

4-Diethylamino-2-(pyridin-2-ylmethoxy)-benzaldehyde (N,N-SP-CHO):

4-(Diethylamino)salicylaldehyde (1 g, 5.18 mmol) and 2-(Chloromethyl)pyridine hydrochloride (0.85 g, 5.18 mmol) was taken in a 50ml round bottom flask and was dissolved in 30ml acetonitrile. After all the reactants had been completely dissolved K_2CO_3 (3.5 g, 25.9 mmol) and tetrabutylammonium iodide (0.95g, 2.5 mmol) was added and the reaction mixture was refluxed for 24 h. After completion of the reaction as confirmed by TLC, acetonitrile was evaporated under reduced pressure. The concentrate was extracted with ethyl acetate, dried over sodium sulphate and vacuum evaporated. The crude mass was purified by flash chromatography using petroleum ether/ ethyl acetate (3:2 v/v) (R_f = 0.5) as eluent to give N,N-SP-CHO as yellowish brown solid 42.8 % (630 mg). ^1H NMR (300 MHz, CDCl_3): δ 10.29 (s, 1H), 8.60-8.58 (dd, J =0.9 Hz, J =4.8 Hz 1H), 7.78-7.71 (m, 2H), 7.62-7.59 (d, J =7.8 Hz, 1H), 7.27-7.22(dd,

$J=3.6$ Hz, $J=10.3$ Hz 1H), 6.31-6.27(dd, $J=2.1$ Hz, $J=9$ Hz, 1H), 6.09-6.08 (d, $J=2.1$ Hz, 1H), 5.31 (s, 2H), 3.40-3.33 (q, $J= 6.9$ Hz, 4H), 1.16-1.11 (t, $J=7.2$ Hz, 6H); ^{13}C NMR (75 MHz, CDCl_3): δ 186.7, 162.5, 156.8, 153.6, 148.9, 148.9, 136.9, 130.8, 122.6, 121.1, 114.1, 104.5, 93.9, 70.5, 44.7, 12.4, 12.4, 12.2 ppm; HRMS-ESI (m/z): calcd for $\text{C}_{17}\text{H}_{21}\text{N}_2\text{O}_2$ $[\text{M}+\text{H}]^+$ 285.1598, found 285.1603.

4-(5,5-difluoro-1,3,7,9-tetramethyl-5H-4 λ^4 ,5 λ^4 dipyrrolo[1,2c:2',1'f][1,3,2]diazaborinin-10-yl)-N,N-diethyl-3-(pyridin-2-ylmethoxy)aniline (N,N-SP-BPY)

2,4-Dimethylpyrrole (368.2 mg, 3.87 mmol) and N,N-SP-CHO (500 mg, 1.76 mmol) were dissolved in dry CH_2Cl_2 (50 mL) under an argon atmosphere. The solution was purged with argon for 10 min followed by addition of Two drops of trifluoroacetic acid (TFA) in the dark. Then the reaction mixture was stirred for 4 h at ambient temperature in the dark. Then 2,3-dichloro-5,6-dicyanoquinone (DDQ, 1.13 g, 2 mmol) was added followed by addition of another 10 mL dry CH_2Cl_2 and the mixture was stirred for another 4 h. Then triethylamine (5 mL) was added to the reaction mixture and stirred for another 5 mins. Then, boron trifluoride etherate (7 mL) was added and the mixture was stirred for another 60 min. The dark brown solution was washed with water (3×20 mL) and brine (30 mL), dried over anhydrous sodium sulfate and concentrated under reduced pressure. The crude product was purified by silica-gel flash column chromatography (EtOAc–petroleum ether, (2.5:7.5 v/v)($R_f = 0.3$) to give N,N-SP-BPY as red solid (283 mg, 32 % yield). ^1H NMR (300 MHz, CDCl_3): δ 8.49-8.48 (d, $J=4.8$ Hz, 1H), 7.57-7.54 (dd, $J=1.5$ Hz, $J=7.8$ Hz 1H), 7.17-7.11 (dd, $J=3.9$ Hz, $J=10$ Hz, 2H), 6.89-6.86 (d, $J=8.4$ Hz, 1H), 6.37-6.34 (dd, $J=2.4$ Hz, $J=8.4$ Hz 1H), 6.30-6.29 (d, $J=2.1$ Hz, 1H), 5.95 (s, 2H), 5.15 (s, 2H), 3.37-3.30 (q, $J= 7.2$ Hz, 4H), 2.56 (s, 6H), 1.57 (s, 6H), 1.15-1.10 (t, $J=6.9$ Hz, 6H); ^{13}C NMR (75 MHz, CDCl_3): δ 157.5, 156.0, 154.1, 149.9, 148.4, 142.7, 140.3, 136.9, 132.5, 129.9, 122.3, 121.0, 120.4, 110.7, 105.1, 96.9, 70.6, 44.4, 36.5, 31.8, 29.6, 29.2, 24.6, 22.6, 14.5, 14.1, 13.9, 12.2 ppm; HRMS-ESI (m/z): calcd for $\text{C}_{29}\text{H}_{33}\text{BFN}_4\text{O}$ $[\text{M}-\text{F}]^+$ 483.2726, found 483.2715. Moreover, the structure of N,N-SP-BPY was confirmed from single crystal X-ray analysis (CCDC 1902075; Figure 1).

2-Benzoyloxy-4-diethylamino-benzaldehyde (N,N-SB-CHO)

4-(Diethylamino) salicylaldehyde (1 g, 5.18 mmol) and Benzyl bromide (0.88 g, 5.18 mmol) was taken in a 50ml round bottom flask and was dissolved in 30ml acetonitrile. After all the reactants had been completely dissolved K_2CO_3 (3.5 g, 25.9 mmol) and tetrabutylammonium iodide (0.95g, 2.5 mmol) was added and the reaction mixture was refluxed for 24 h. After completion of the reaction as confirmed by TLC, acetonitrile was evaporated under reduced pressure. The

concentrate was extracted with ethyl acetate, dried over sodium sulphate and vacuum evaporated. The crude mass was purified by flash chromatography using petroleum ether/ ethyl acetate (4:1 v/v) ($R_f = 0.5$) as eluent to give N,N-SB-CHO as yellowish white solid 49 % (728 mg).

^1H NMR (300 MHz, CDCl_3): δ 10.25 (s, 1H), 7.76-7.73 (d, $J=9$ Hz, 1H), 7.47-7.31 (m, 5H), 6.31-6.28 (d, $J=8.7$ Hz, 1H), 6.07-6.06 (d, $J=2.1$ Hz, 1H), 5.18 (s, 2H), 3.42-3.35 (q, $J=6.9$ Hz, 4H), 1.19-1.44 (t, $J=6.9$ Hz, 6H); ^{13}C NMR (75 MHz, CDCl_3): δ 186.8, 163.3, 153.8, 136.8, 130.3, 128.7, 128.6, 128.3, 127.9, 127.1, 127.0, 126.9, 126.9, 114.4, 104.6, 94.2, 70.0, 44.8, 44.7, 12.5, 12.5 ppm; HRMS-ESI (m/z): calcd for $\text{C}_{18}\text{H}_{22}\text{NO}_2$ $[\text{M}+\text{H}]^+$ 284.1645, found 284.1645.

3-(benzyloxy)-4-(5,5-difluoro-1,3,7,9-tetramethyl-5H-4 λ^4 ,5 λ^4 -dipyrrolo[1,2-c:2',1'-f][1,3,2]diazaborinin-10-yl)-N,N-diethylaniline (N,N-SB-BPY)

2,4-Dimethylpyrrole (368.2 mg, 3.87 mmol) and N,N-SB-CHO (500 mg, 1.76 mmol) were dissolved in dry CH_2Cl_2 (50 mL) under an argon atmosphere. The solution was purged with argon for 10 min followed by addition of Two drops of trifluoroacetic acid (TFA) in the dark. Then the reaction mixture was stirred for 4 h at ambient temperature in the dark. Then 2,3-dichloro-5,6-dicyanoquinone (DDQ, 1.13 g, 2 mmol) was added followed by addition of another 10 mL dry CH_2Cl_2 and the mixture was stirred for another 4 h. Then triethylamine (5 mL) was added to the reaction mixture and stirred for another 5 mins. Then, boron trifluoride etherate (7 mL) was added and the mixture was stirred for another 60 min. The dark brown solution was washed with water (3×20 mL) and brine (30 mL), dried over anhydrous sodium sulfate and concentrated under reduced pressure. The crude product was purified by silica-gel flash column chromatography (EtOAc–petroleum ether, (0.75:4.25 v/v) ($R_f = 0.4$) to give N,N-SB-BPY as red solid (204 mg, 22.3% yield). ^1H NMR (300 MHz, CDCl_3): δ 7.19-7.13 (m, 5H), 6.79-6.76 (d, $J=8.4$ Hz 1H), 6.28-6.25 (dd, $J=2.4$ Hz, $J=8.5$ Hz, 1H), 6.17-6.16 (d, $J=2.1$ Hz, 1H), 5.89 (s, 2H), 4.98 (s, 2H), 3.27-3.20 (q, $J=6.9$ Hz, 4H), 2.49 (s, 6H), 1.49 (s, 6H), 1.06-1.04 (t, $J=5.1$ Hz, 6H); ^{13}C NMR (75 MHz, CDCl_3): δ 156.4, 154.1, 149.9, 142.9, 140.5, 137.6, 132.6, 129.9, 128.5, 157.6, 126.7, 120.5, 111.3, 105.3, 97.8, 92.1, 70.1, 44.5, 36.2, 29.7, 28.5, 24.7, 23.8, 23.4, 17.3, 14.6, 14.2, 12.4, 7.9 ppm; HRMS-ESI (m/z): calcd for $\text{C}_{30}\text{H}_{35}\text{BF}_2\text{N}_3\text{O}$ $[\text{M}+\text{H}]^+$ 502.2836, found 502.2835.

3-(benzyloxy)-4-(5,5-difluoro-1,3,7,9-tetramethyl-5H-4 λ^4 ,5 λ^4 -dipyrrolo[1,2-c:2',1'-f][1,3,2]diazaborinin-10-yl)-N,N-diethylaniline (N,N-SB-BPY)

2,4-Dimethylpyrrole (368.2 mg, 3.87 mmol) and N,N-SB-CHO (500 mg, 1.76 mmol) were dissolved in dry CH_2Cl_2 (50 mL) under an argon atmosphere. The solution was purged with argon for 10 min followed by addition of Two drops of trifluoroacetic acid (TFA) in the dark. Then the

reaction mixture was stirred for 4 h at ambient temperature in the dark. Then 2,3-dichloro-5,6-dicyanoquinone (DDQ, 1.13 g, 2 mmol) was added followed by addition of another 10 mL dry CH_2Cl_2 and the mixture was stirred for another 4 h. Then triethylamine (5 mL) was added to the reaction mixture and stirred for another 5 mins. Then, boron trifluoride etherate (7 mL) was added and the mixture was stirred for another 60 min. The dark brown solution was washed with water (3×20 mL) and brine (30 mL), dried over anhydrous sodium sulfate and concentrated under reduced pressure. The crude product was purified by silica-gel flash column chromatography (EtOAc–petroleum ether, (0.75:4.25 v/v) ($R_f = 0.4$) to give N,N-SB-BPY as red solid (204 mg, 22.3% yield). ^1H NMR (300 MHz, CDCl_3): δ 7.19-7.13 (m, 5H), 6.79-6.76 (d, $J=8.4$ Hz 1H), 6.28-6.25 (dd, $J=2.4$ Hz, $J=8.5$ Hz, 1H), 6.17-6.16 (d, $J=2.1$ Hz, 1H), 5.89 (s, 2H), 4.98 (s, 2H), 3.27-3.20 (q, $J= 6.9$ Hz, 4H), 2.49 (s, 6H), 1.49 (s, 6H), 1.06-1.04 (t, $J=5.1$ Hz, 6H); ^{13}C NMR (75 MHz, CDCl_3): δ 156.4, 154.1, 149.9, 142.9, 140.5, 137.6, 132.6, 129.9, 128.5, 157.6, 126.7, 120.5, 111.3, 105.3, 97.8, 92.2, 70.1, 44.5, 36.2, 29.7, 28.5, 24.7, 23.8, 23.4, 17.3, 14.6, 14.2, 12.4, 7.9 ppm; HRMS-ESI (m/z): calcd for $\text{C}_{30}\text{H}_{35}\text{BF}_2\text{N}_3\text{O}$ $[\text{M}+\text{H}]^+$ 502.2836, found 502.2835.

5,5-difluoro-1,3,7,9-tetramethyl-10-(2-(pyridin-2-ylmethoxy)phenyl)-5H-4 λ^4 ,5 λ^4 -dipyrrolo[1,2-*c*:2',1'-*f*][1,3,2]diazaborinine (SP-BPY)

2,4-Dimethylpyrrole (473 mg, 4.97mmol) and SP-CHO (530 mg, 2.48mmol) were dissolved in dry CH_2Cl_2 (50 mL) under an argon atmosphere. The solution was purged with argon for 15 min followed by addition of Two drops of trifluoroacetic acid (TFA) in the dark. Then the reaction mixture was stirred for 4 h at ambient temperature in the dark. Then 2,3-dichloro-5,6-dicyanoquinone (DDQ, 613 mg, 2.7mmol) was added followed by addition of another 10 mL dry CH_2Cl_2 and the mixture was stirred for another 4 h. Then triethylamine (5 mL) was added to the reaction mixture and stirred for another 5 mins. Then, boron trifluoride etherate (7 mL) was added and the mixture was stirred for another 60 min. The dark brown solution was washed with water (3×20 mL) and brine (30 mL), dried over anhydrous sodium sulfate and concentrated under reduced pressure. The crude product was purified by silica-gel flash column chromatography (EtOAc–petroleum ether, (1:4) v/v) ($R_f = 0.2$) to give SP-BPY as red solid (268 mg, 25 % yield). ^1H NMR (300 MHz, CDCl_3): δ 8.56-8.55 (d, $J=5.4$ Hz, 1H), 7.66-7.62 (t, $J= 7.8$ Hz, 1H), 7.49-7.44 (t, $J=8.1$ Hz, 1H), 7.26-7.11 (m, 5H), 6.02 (s, 2H), 5.26 (s, 2H), 2.63 (s, 6H), 1.48 (s, 6H); ^{13}C NMR (75 MHz, CDCl_3): δ 156.9, 155.2, 155.1, 148.5, 142.6, 138.8, 137.2, 131.58, 130.8, 129.6, 124.4, 122.7, 122.1, 121.1, 120.9, 113.2, 70.9, 29.7, 14.6, 14.1, 13.9 ppm; HRMS-ESI (m/z): calcd for $\text{C}_{25}\text{H}_{24}\text{BFN}_3\text{O}$ $[\text{M}-\text{F}]^+$ 412.1991, found 412.2025.

3. Results and Discussion

The recognition of anionic substrates by positively charged or electrically neutral receptor systems has emerged as an area of active research owing to their definite roles in complex biological systems. In a receptor-based approach, it is very important to design the receptor such a way that appropriate positions should be available for effective synergistic binding. The binding between receptors and the amino acid guests are usually strong enough viz. H-bonding or covalent bonding to observe photophysical changes of receptor upon binding with guests. In the present investigation, we have chosen functionalized BODIPY as an acceptor/receptor for amino acid binding. BODIPY dyes are often used for recognition of anionic substrates including amino acids [46-50]. Asp and Glu are carboxylic acids and therefore difficult to design receptor for these amino acids to obtain covalent type bonding [51-53]. We have carefully chosen N,N-diethylamino benzaldehyde as starting material for designing of these probes. Introduction of the picolyl group at a suitable position makes perfect space for amino acids like Asp or Glu to form simultaneous H-bonding. A theoretical calculation was performed to support the designing strategy of the probe. In accordance with H-bonding principle, it is very important to have N donor sites for the carboxylate group. The interaction between 'N' centre and Asp or Glu has been strong enough to attain photophysical changes in the probe.

3.1. Fluorescence and absorption spectral studies

The Probe **N,N-SP-BPY** is weakly emissive due to an effective PET process. It showed an emission maximum at 527nm as shown in Figure 1. Upon addition of Asp or Glu, the band at 527 nm increases rapidly upon excitation at 450 nm. This band was attributed from the blocking of the PET process. Initially, a possible PET process was initiated from 'N' centre of N,N-diethylamino moiety to BODIPY core unit. Upon addition of Asp or Glu, the 'N' center gets involved in weak H-bonds with amino acid inhibiting the PET process leading to an increase in emission band at 527 nm (Figure 2). Therefore, the probe **N,N-SP-BPY** senses Asp or Glu as a result of inhibition of the PET process.

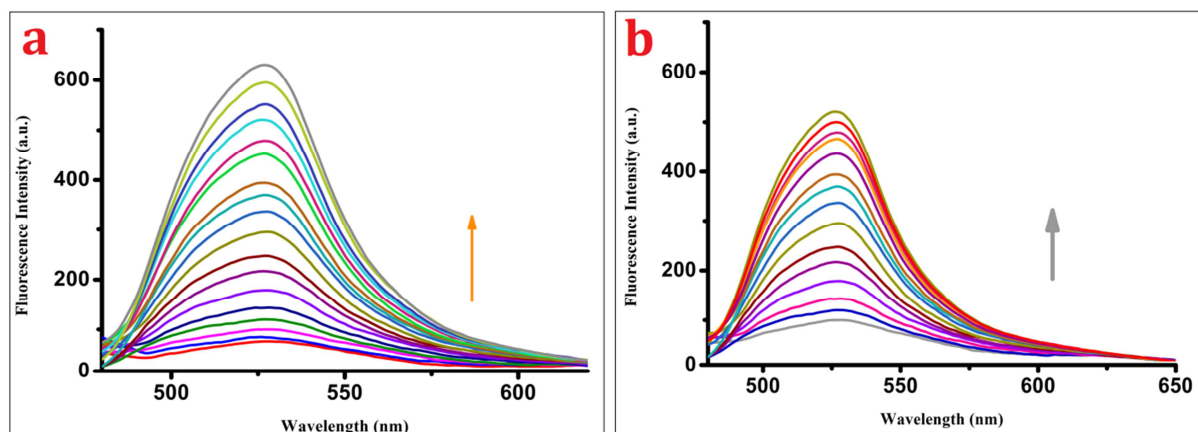


Figure 2: Changes in the emission spectra of *N,N*-SP-BPY (20 μ M) upon gradual addition of (a) Asp (0-600 μ M) and (b) Glu (0-600 μ M) in 3:97 DMSO:H₂O (v/v; pH 6.5 ; λ_{ex} 450 nm).

On the other hand, *N,N*-SP-BPY has four absorbance bands centered at 268nm, 309nm, 376nm, and 514nm respectively. All the absorbance bands were decreased simultaneously upon addition of Asp or Glu. Interestingly, the main absorbance band at 514nm was blue shifted to 503 nm with the addition of increasing amount of either amino acid (Figure 3). The corresponding naked eye color of the solution was altered from pink to colorless (Figure 4).

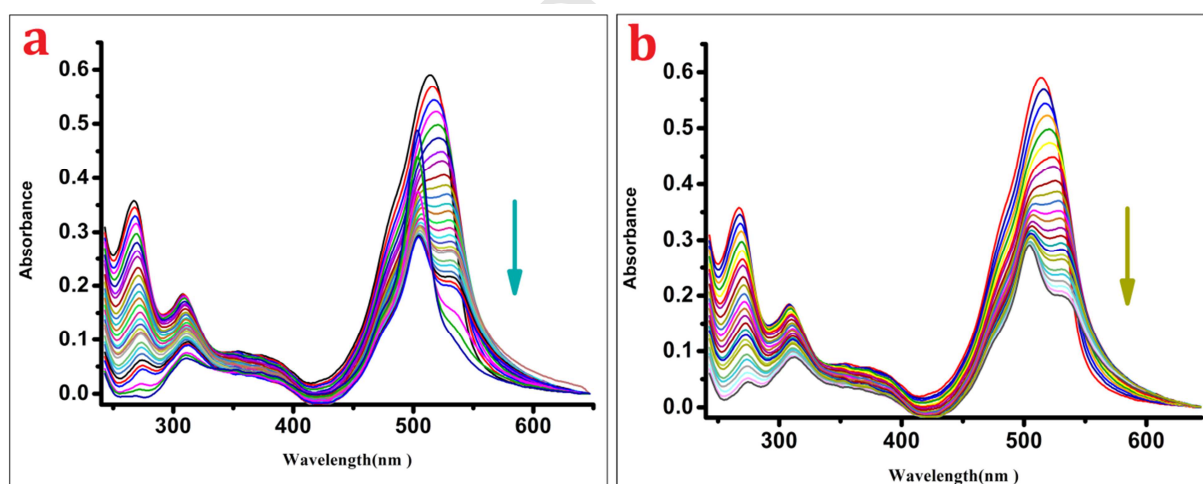


Figure 3: Changes in the absorbance spectra of *N,N*-SP-BPY (20 μ M) upon gradual addition of (a) Asp (0-600 μ M) and (b) Glu (0-600 μ M) in 3: 97 DMSO: H₂O (v/v; pH 6.5).

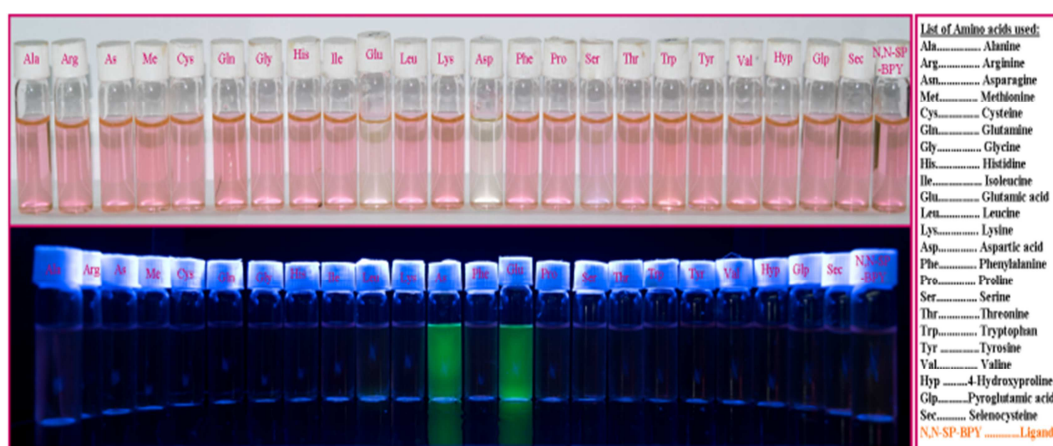


Figure 4: Naked eye and UV light exposed color change of **N,N-SP-BPY** (20 μM) in the presence of different amino acids up to 600 μM .

From Job's plot a 1:1 binding interaction was observed between probe **N,N-SP-BPY** and its adduct with Asp (Figure S-18, ESI). In order to establish the selectivity of the probe for Asp and Glu, a competitive UV-Vis and fluorescence measurement experiments were performed. Except for Asp and Glu, amino acids like Ala, Arg, Asn, Gln, Gly, His, Ile, Leu, Lys, Met, Phe, Pro, Ser, Thr, Trp, Tyr, Val, Glp, Sec didn't significantly alter the fluorescence profile of **N,N-SP-BPY** (Figure 5). Amino acid Cys enhanced the emission maxima only by a small degree. Similarly, only Asp and Glu was found to draw a change in absorbance profile of the probe (Figure 6). The emission intensity of the probe **N,N-SP-BPY** did not change significantly in the presence of other amino acids in the same sample (Figure S-19, ESI). A relative plot of the emission intensity of **N,N-SP-BPY** in the presence of other amino acids has been incorporated in Figure S-19. A comparison table has also been incorporated on fluorescent probes found in the literature for Asp and Glu (Table S-1, ESI) to validate the effectiveness of the probe. Most of the reported probes in the table lacks selectivity, and have a poor quantum yield in the biological system. The probe can selectively detect Asp/Glu in a mixture of a sample containing each amino acid.

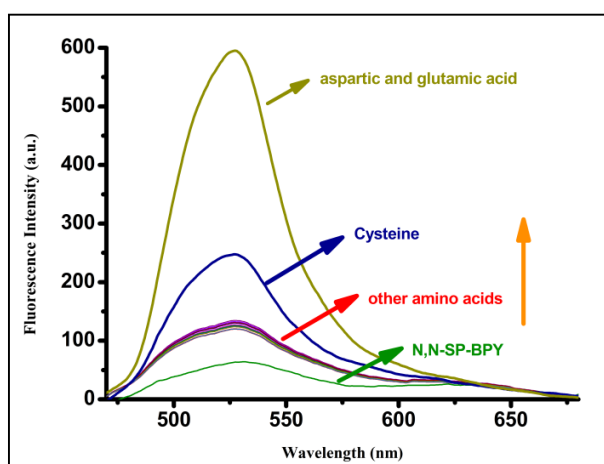


Figure 5: Changes in the fluorescence profile of **N,N-SP-BPY** (20 μM) upon gradual addition of all other amino acids up to 600 μM in 3:97 DMSO: H_2O (v/v; pH 6.5).

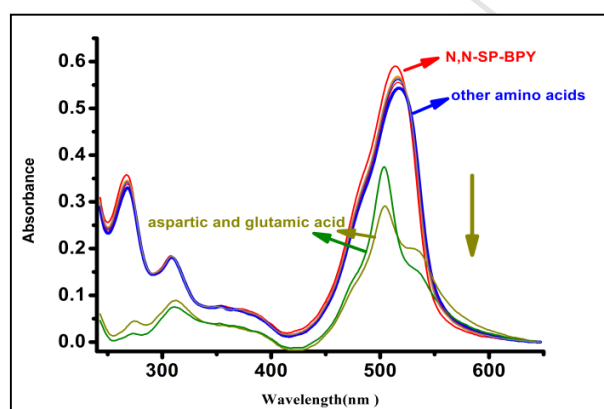


Figure 6: Changes in the absorbance spectra of **N,N-SP-BPY** (20 μM) upon gradual addition of all other amino acids up to 500 μM in 3: 97 DMSO: H_2O (v/v; pH 6.5).

Furthermore, we had synthesized 2 model compounds **N,N-SB-BPY**, and **SP-BPY** (scheme-1) to understand the observed PET process. In **N,N-SB-BPY** the picolyl group of probe **N,N-SP-BPY** was replaced by simple a benzyl group and **SP-BPY** has no **N,N**-diethylamino group. Initially, we have expected two possible PET to be active in the probe **N,N-SP-BPY**, one operating from **N,N**-diethylamino group and another from the picolyl group to BODIPY core unit. So the fluorescence and UV-Vis changes of these two model compounds were investigated. **N,N-SB-BPY** was weakly fluorescent indicating a PET process was indeed active from **N,N**-diethylamino group to BODIPY

core. The emission maximum was situated at 524nm and upon addition of either Asp/Glu the emission maxima increases and shifted slightly to 527nm (Figure 7a).

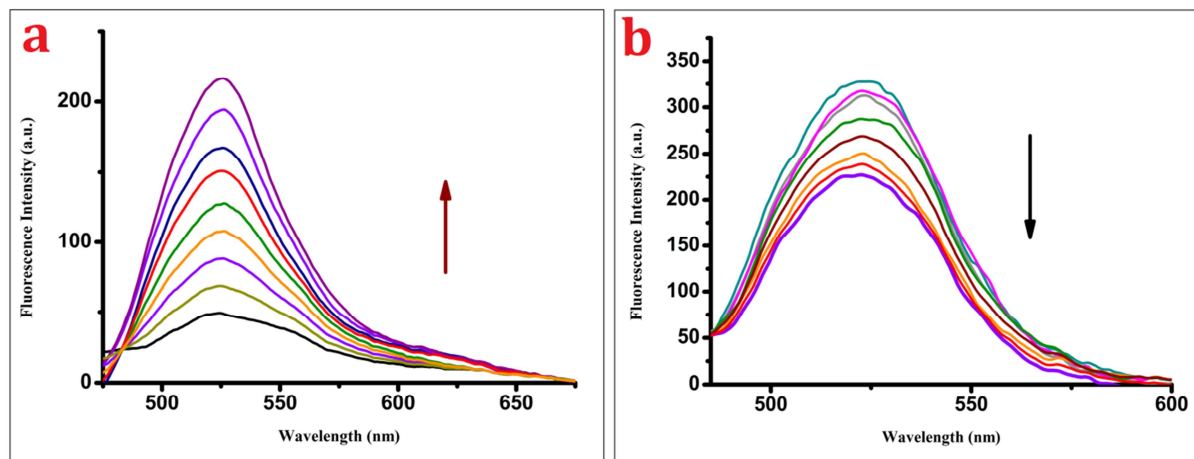


Figure 7. Changes in the fluorescence spectra following addition of Asp (0-600 μM) in (a) **N,N-SB-BPY** (20 μM) and (b) **SP-BPY** in 3:97 DMSO: H₂O (pH v/v; pH 6.5)

On the other hand, the emission intensity of **SP-BPY** (524nm, λ_{ex} 450 nm) decreases upon addition of Asp or Glu (Figure 7b).

Therefore, we concluded that only one PET was operating in the probe **N,N-SP-BPY**. On the other hand, PET process between a receptor and suitable electron donating moieties viz. amino acid or anion, can quench fluorescence upon van der Waals contact and supports molecular contact. Hence, it can be concluded that there must have van der Waals contact or H-bonding interaction between the picolyl group of **SP-BPY** and the amino acid.

Hence, we concluded that the fluorescence enhancement of the probe **N,N-SP-BPY** arise due to quenching of PET and the picolyl group was introduced to have a van der Waals contact or H-bonding interaction between the ligand and amino acid.

Furthermore, UV-Vis changes of **N,N-SB-BPY**, and **SP-BPY** were carried out in the presence of Asp. The main absorbance peak of **N,N-SB-BPY** was centered at 270 nm, 309 nm, 518nm respectively (Figure 8). Upon addition of Asp or Glu, the entire absorbance band decreased continuously. Similarly, the main characteristic absorbance band of **SP-BPY** at 388 nm, 501nm, and 539 nm also decreased in the presence of either amino acid. Therefore, a strong case of H-bonding interaction may be proposed.

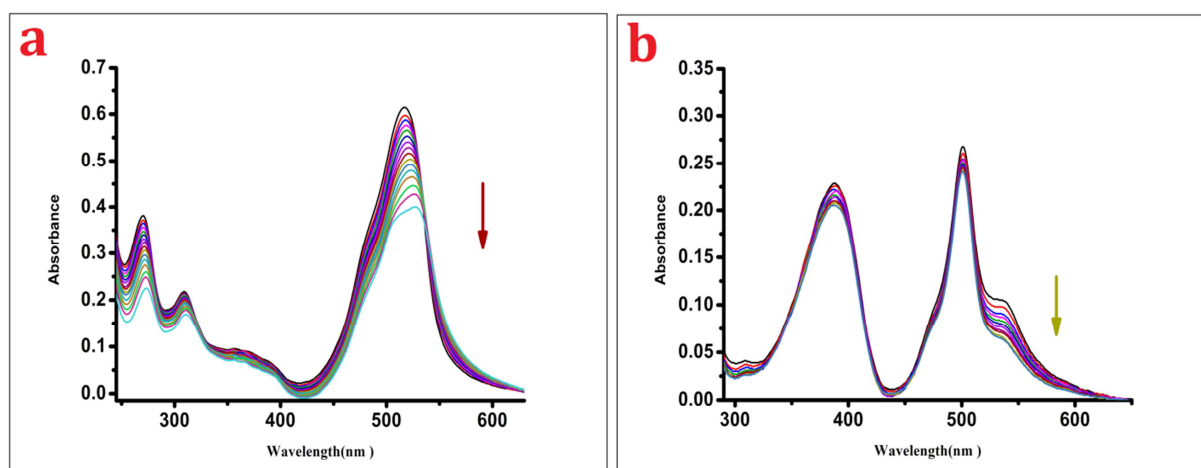


Figure 8: Changes in the Absorbance profile following addition of Asp (0-600 μM) in (a) **N,N-SB-BPY** (20 μM) and (b) **SP-BPY** in 3: 97 DMSO: H_2O (v/v; pH 6.5)

The lowest detection limit of **N,N-SP-BPY** as calculated from fluorescence intensity was found to be 1 μM and 5 μM (ESI) for Asp and Glu respectively. In the plot of emission intensity vs. Asp concentration, the linear region (up to 10 μM Asp) was useful for the determination of an unknown concentration of Asp (Figure S-20, ESI). The quantum yield of the probe **N,N-SP-BPY** and its adduct with Asp was found to be 0.031 and 0.130. The association constant of probe for Asp was estimated to be $1.49 \times 10^5 \text{ M}^{-1}$ from fluorescence titration using modified Benesi-Hildebrand equation [54], $(F_{\text{max}} - F_0) / (F_x - F_0) = 1 + (1/K)(1/[M]_n)$, where F_{max} , F_0 , and F_x are fluorescence intensities of **N,N-SP-BPY** in the presence of Asp at saturation, free **N,N-SP-BPY**, and any intermediate Asp concentration (Figure S-21, ESI).

3.2. Influence of pH

At different pH range (pH 2.0-8.0), the emission intensity of **N,N-SP-BPY** in the presence and in the absence of Asp and Glu was thoroughly investigated (Figure 9). The supporting data clearly indicated that the difference in emission intensities of **N,N-SP-BPY** and its complex with Asp/Glu was significant at pH 6.5. Hence, all the experiments were carried at pH 6.5 buffer system. From figure 9, it can be seen that the probe is non-fluorescent in the pH range 5-8 due to the active PET process. However, at low pH range 2-4, protonation at the N center of N, N-diethyl moiety occurs and subsequently, the observed PET is inhibited, resulting in strong fluorescence. In pH range 6-6.5, Aspartic acid remains in di-anionic form, thus participating in two simultaneous H-bonds with the probe. With an increase in pH, the H-bonding probability decreases and therefore, no emission could be observed. Lowering the pH to 5, the anionic form of $\beta\text{-COOH}$ disappears and therefore no fluorescence can be observed.

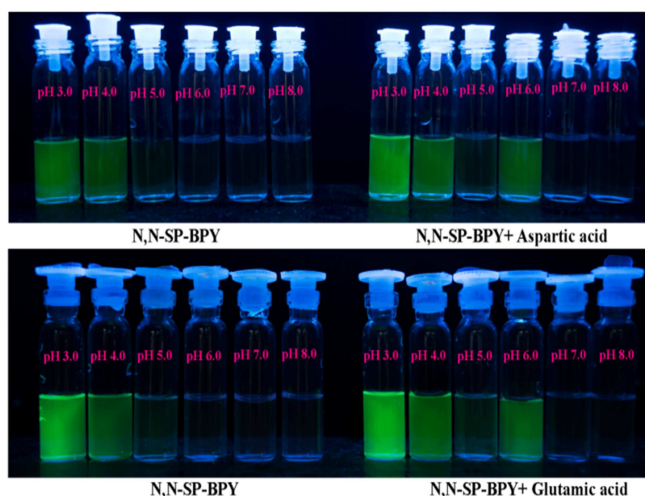


Figure 9: Change in emission intensity of N,N-SP-BPY and its complex with Asp and Glu at different pH.

3.3. Mode of sensing between N,N-SP-BPY and Asp/Glu

The possible sensing mechanism of N,N-SP-BPY with Asp/Glu which lead to the change in absorbance and fluorescence profile were shown in Figure 10. Asp and Glu form two simultaneous H-bonds with the nitrogen of N, N-diethylamino and picolyl unit, inhibiting the PET process. Hence strong fluorescence was observed.

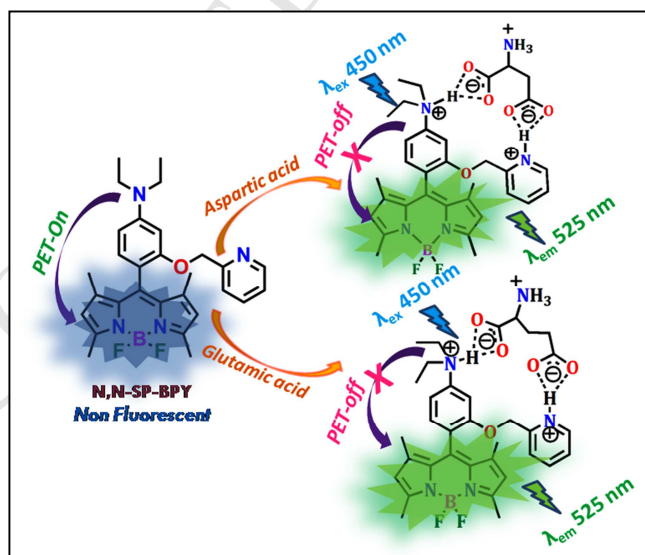


Figure 10. Possible binding mechanism of Asp and Glu with N,N-SP-BPY

In order to discriminate the PET process with competing ICT, we have measured the fluorescence and absorbance of **N,N-SP-BPY** in different organic solvent systems (Figure S-22, S-23). The most prominent distinction between PET and ICT sensors lies in the different fluorescence response upon analyte recognition. PET probes display fluorescence enhancement or quenching without pronounced spectral shifts so that the terms 'off-on' and 'on-off' fluorescent sensors are often used. In contrast, indicators based on ICT show clear fluorescence band shifts upon analyte binding, making ratiometric measurements possible.

Our probe **N,N-SP-BPY** satisfies the perpendicular arrangement of the fluorophore and the chelator, as seen from the crystal structure of the ligand. From S-22, S-23, it could be clearly seen that the λ_{max} UV varies between 500-503 nm and λ_{max} FI from 526-535 nm. Therefore, the sensing mechanism is based on the inhibition of PET rather than ICT.

In order to gain further insight into the mechanistic aspect of sensing of the probe **N,N-SP-BPY**, $^1\text{H-NMR}$ titrations were performed using $\text{CD}_3\text{CN-}d_4\text{:D}_2\text{O}$ (4:1). On adding Aspartic acid, a downfield shift was observed in the proton signal of (b), which is present in the para position of nitrogen atom of the pyridine ring. The value shifts from δ 7.62 to 7.64 (Figure 11), clearly indicating interaction between the pyridine nitrogen and the hydrogen of carboxylic acid moiety present in the analyte (Figure 10). The proton (a) upfield shifted from 8.51 to 8.44. In the free ligand, the protons present in the meta position (c) and (d) were merged together where as in the complex they were separated and downfield shifted from δ 7.22 to 7.325 (c) and from upfield δ 7.12 to 7.09. Protons present in the N,N-diethyl benzene part of the ligand was also affected, indicating interaction between nitrogen of the benzene ring and the analyte. Protons (e, f and g) of N,N-diethyl aromatic moiety was upfield shifted from δ 6.91 to 6.90, δ 6.44 to 6.33 and from δ 6.41 to 6.39. Interaction with the analyte also affects the electron density over the BODIPY core as indicated by slight upfield shift of the pyrrole protons (i, i') from δ 6.08 to 6.07 and 5.16 to 5.14. As the electron density of the nitrogen atom of N,N-diethyl moiety changes the CH_2 (k) and CH_3 (j) protons was also shifted from δ 3.37 to 3.34 and from δ 1.11 to 1.05 (Figure 10). Similar trend was also observed when $^1\text{H-NMR}$ titration was carried out in $\text{MeOH-}d_4\text{:D}_2\text{O}$ (4:1); to support the binding mechanism between Asp/Glu acid and **N,N-SP-BPY** (Figure S-24, ESI and Table S-3 to S-4). Thus $^1\text{H-NMR}$ titration evidently supports our mechanistic proposal. All the significant changes in $^1\text{H NMR}$ of **N,N-SP-BPY** have been shown in Table S-2 to S-4, ESI.

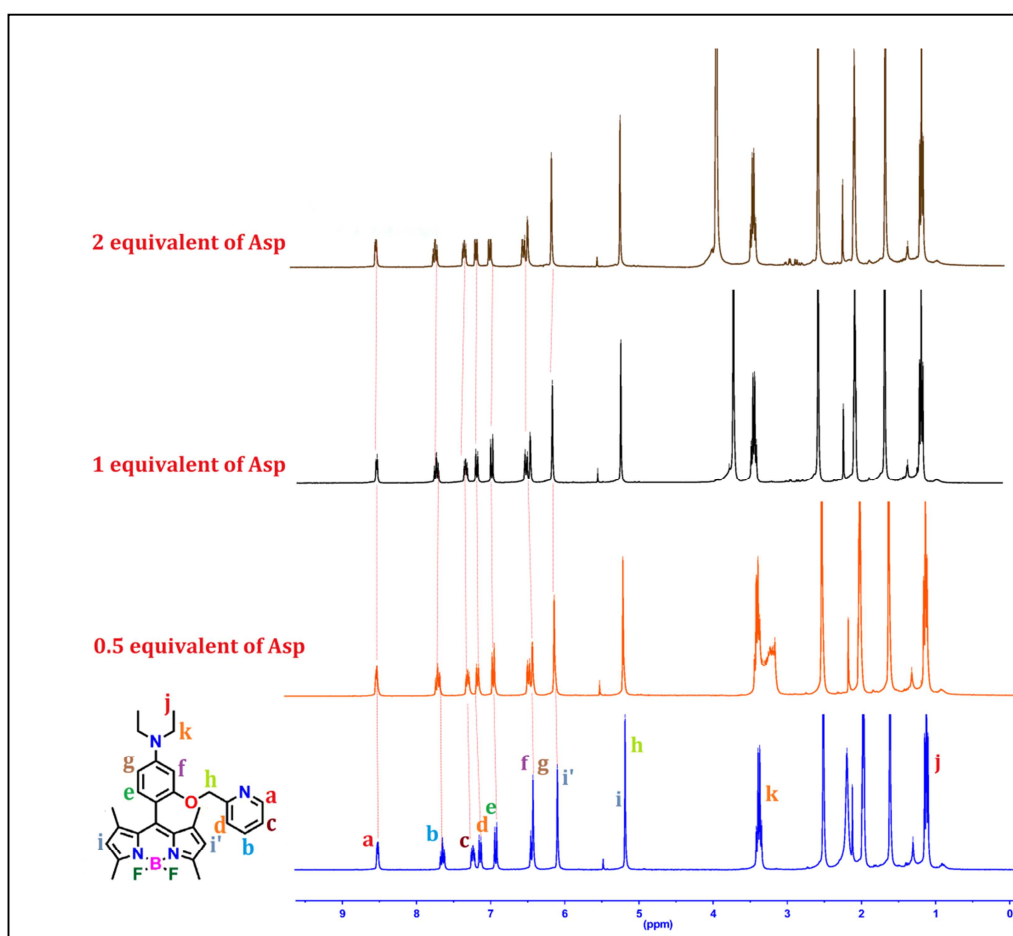


Figure 11. ^1H NMR titration of **N,N-SP-BPY** in $\text{CD}_3\text{CN}-d_4:\text{D}_2\text{O}$ (3:1); Shift of aromatic protons upon addition of increasing amount of Asp (0, 0.5, 1, 2 equivalent respectively).

3.4. Theoretical calculations

For the purpose of understanding the sensing mechanism and to attain a better picture of the molecular orbital framework, structural optimization of **N,N-SP-BPY** and its complex with Aspartic and Glutamic acid was carried out using density functional theory (DFT) as implemented in Gaussian 09 software [55]. Becke's three-parameter hybrid functional with the LYP correlation functional (B3LYP) was used with the 6-31G(d,p) basis set for geometry optimization in water using conductor-like polarizable continuum model (C-PCM) as a solvent model.

The ground state optimized structure of **N,N-SP-BPY** revealed localization of HOMO on N,N diethyl benzene moiety while the LUMO is localized on BODIPY core (Figure 12). This suggests a strong photoinduced electron transfer (PET) process acting between BODIPY core and N,N diethyl benzene unit. Therefore no fluorescence could be expected for **N,N-SP-BPY**. The HOMO

and LUMO of **N,N-SP-BPY** has the energy of -5.163 eV and -2.463 eV respectively with an energy difference of 2.7 eV (459 nm).

Addition of Asp or Glu results in the formation of hydrogen-bonded complexes in which both the HOMO and LUMO are located in BODIPY core. Therefore, the active PET process occurring in the ligand was inhibited, and strong green fluorescence was observed. The nitrogen atom of *N,N*-diethylamino, and the picolyl unit take part in hydrogen bonding interaction with respective amino acids. The energy of HOMO and LUMO for the complex with Asp was found to be -5.562 eV and -2.561 eV, and for Glu -5.532 eV and -2.532 eV respectively. The energy difference in both the complex was found to be 3.0 eV (413 nm). Hence, *N,N*-SP-BPY could form a stable complex with Asp and Glu (Figure 11). Furthermore, theoretical, as well as experimental studies depict the blue shift in UV-visible spectra. All the HOMO-LUMO energy levels and optimized structures are shown in table S-5 to S-7, ESI.

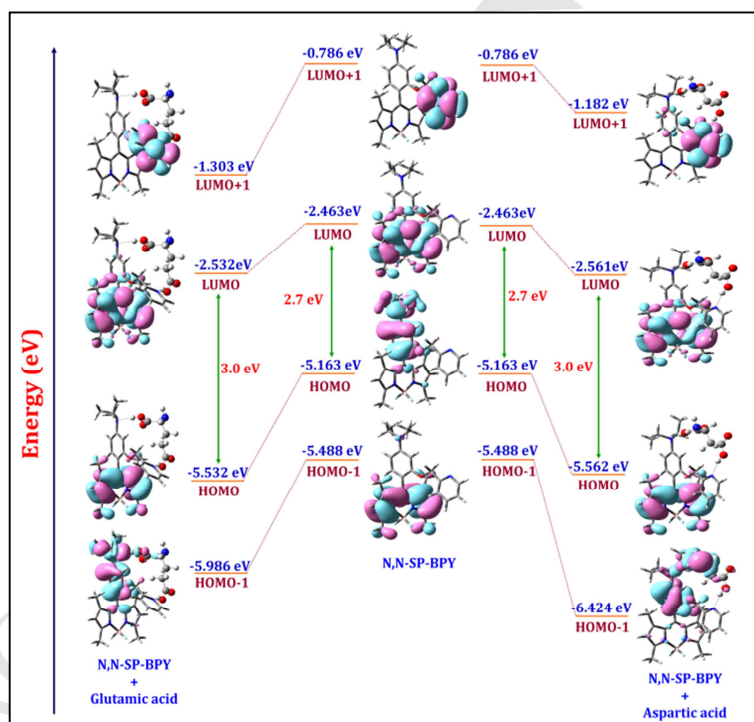


Figure 12: HOMO-LUMO energy gaps in *N,N*-SP-BPY Aspartic acid and Glutamic acid in Water.

3.5. Intracellular imaging study

Imaging experiments were conducted for fluorescent visualization of intracellular Asp and Glu in live HeLa, MDA-MB-468, A549 and HEK 293T cell lines. Cells were incubated in presence of 20 μ M of probe **N,N-SP-BPY** for 2 hours (h) at 37⁰C and 5% CO₂ in the culture medium. After

washing with PBS ($\times 3$), to remove the remaining probe, the cells were incubated with 50 μM of each amino acid for another 1hour. The cells were then washed with PBS ($\times 2$), and fluorescent images of the cells were collected.

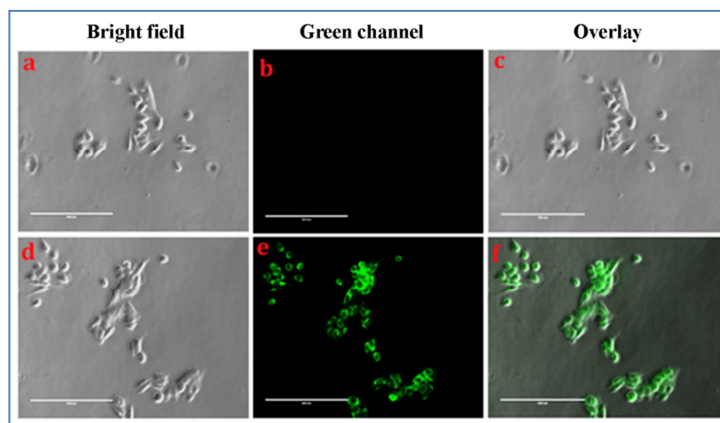


Figure 13: Representative fluorescent images of MDA-MB-468 cells exposed to (a) cells incubated with 20 μM of **N,N-SP-BPY**; (b) green channel images of (a); (c) Overlay of (a) and (b); (d) Images were taken after incubation with 20 μM of **N,N-SP-BPY** and followed by 1hour incubation with Asp (e) green channel image of (d); (f) Overlay of (d) and (e). The cells were visualized under a fluorescence microscope; EVOS FL Cell Imaging System equipped with Plan Fluor, 20X, NA 0.75 objective (Life Technologies), USA; (scale bar 200 μm).

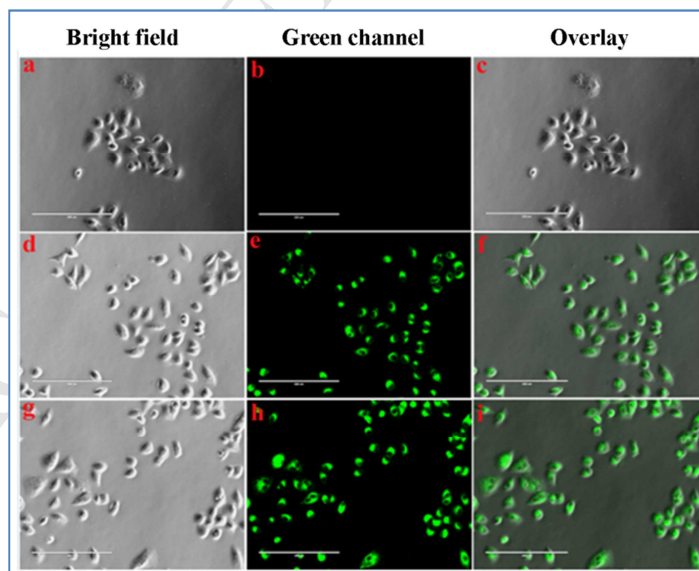


Figure 14: Imaging of Asp/Glu in A549 cells: (a) bright field image of cells after incubating with **N,N-SP-BPY** (20 μM); (b) green channel image of the cells; (c) Overlay of (a) and (b); (d) bright field image of the cells after incubation with **N,N-SP-BPY** (20 μM) and followed by 50 μM Asp; (e) green channel

image of (d) ; (f) Overlay of (d) and (e); (g) bright field image of the cells after incubation with **N,N-SP-BPY** (20 μM) and followed by 50 μM Glu (h) green channel image of (g); (i) Overlay of (g) and (h); (scale bar 200 μm).

No fluorescence was observed in cells (control cells; Figure 13b, 14b and 15b) that were not previously exposed to either Asp or Glu. Cells that were incubated for 1 hr with either of the amino acids showed a significant enhancement of fluorescence in the green channel.

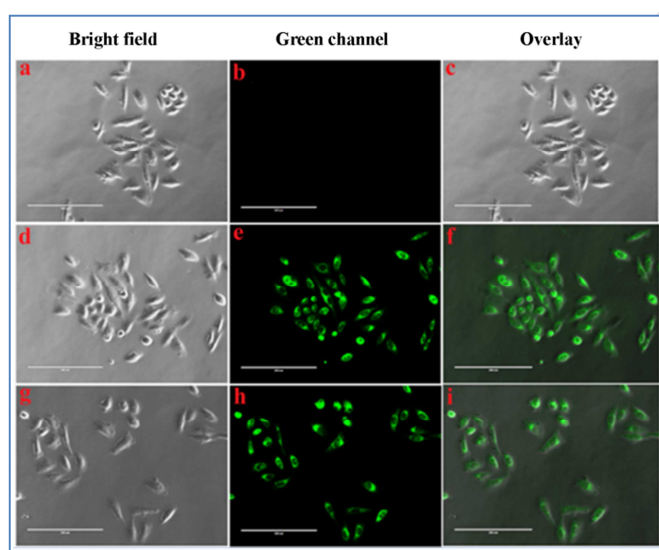


Figure 15: Imaging of Asp/Glu in HeLa cells: (a) bright field image of cells after incubating with **N,N-SP-BPY** (20 μM); (b) green channel image of the cells; (c) Overlay of (a) and (b); (d) bright field image of the cells after incubation with **N,N-SP-BPY** (20 μM) and followed by 50 μM Asp; (e) Green channel image of (d) ; (f) Overlay of (d) and (e); (g) bright field image of the cells after incubation with **N,N-SP-BPY** (20 μM) and followed by 50 μM Glu; (h) Green channel image of (g); (i) Overlay of (g) and (h); (scale bar 200 μm).

Figure 13-15 showed that the probe **N,N-SP-BPY** is cell permeable and can bind to the free Asp or Glu in the cellular system. **N,N-SP-BPY** is highly stable in the cellular system, and over a range of different pH. The difference in emission intensity between the probe and its complex with either amino acid was significant enough to carry out any cellular imaging studies. Furthermore, we have carried out cell imaging experiment in normal HEK-293T cell line. Figure S-26 showed that **N,N-SP-BPY** is highly an efficient biomarker for imaging intracellular Asp/Glu in normal cells without any significant cytotoxic effect.

In order to examine the efficiency of the probe in detecting Asp/Glu at different pH values, we have performed a pH-dependent fixed cell imaging experiment with **N,N-SP-BPY** in presence of Asp. The result showed that maximum background-free fluorescence intensity could be achieved in the range of biological pH (Figure S-27).

Therefore, the probe can be used as a biomarker for the detection of free Asp/Glu in different cancer as well as in normal cell lines. The cytotoxicity of the probe on HeLa cells was determined by MTT assay (Figure S-28). The result showed that upon treatment with 20 μ M of **N,N-SP-BPY** for 12hrs, almost 90% of the cells remains viable, indicating the non-toxic nature of ligand. Hence, the concentration of probe has been fixed to 20 μ M in all experiments. Therefore, **N,N-SP-BPY** may be used as an effective probe for detection of Asp or Glu in living systems.

4. Conclusions

In summary, we have designed and synthesized BODIPY based excellent colorimetric and fluorescence probe **N,N-SP-BPY** for selective detection of Asp/Glu in water. The probe detects Asp/Glu to a concentration as low as 1 μ M and 5 μ M respectively. **N,N-SP-BPY** effectively images intracellular Asp/Glu in A549, HeLa, MDA-MB-468 and normal HEK-293T cells. Furthermore, the cellular imaging studies clearly suggest that probe **N,N-SP-BPY** has good cell permeability and shows better selectivity towards Asp/Glu ions. Fluorescence microscopic study shows intracellular fluorescence emission through the formation of the **N,N-SP-BPY** Asp/Glu complex.

Conflicts of interest

There are no conflicts of interest

Acknowledgements

S.G, acknowledges CSIR for fellowship. A.G and A.A acknowledges DST Nano Mission. S.A acknowledges SERB-DST, New Delhi, India, project No. EMR/2017/002140 for funding. We acknowledge Mr. Arghyadeep Bhattacharyya for helping us with X-ray crystallography studies.

Notes and references

- 1 Pradhan T, Jung HS, Jang JH, Kim TW, Kang C, Kim, JS. Chemical sensing of neurotransmitters. Chem Soc Rev 2014; 43:4684-4713.

- 2 Skvortsova VI, Raevskii KS, Kovalenko AV, Kudrin VS, Malikova LA, Sokolov MA, Alekseev AA, Gusev EI. Levels of neurotransmitter amino acids in the cerebrospinal fluid of patients with acute ischemic insult. *Neurosci Behav Physiol* 2000; 30: 491-495.
- 3 Curtis DR, Johnston GAR. Amino acid transmitters in the mammalian central nervous system. *ErgebPhysiol* 1974; 69: 97-188.
- 4 Johnson JL. Aspartic acid as a precursor for glutamic acid and glycine. *Brain Res* 1974; 67: 358-362.
- 5 Owen OE, Kalhan SC, Hanson RW, The Key Role of Anaplerosis and Cataplerosis for Citric Acid Cycle Function. *J Biol Chem* 2002; 34: 30409-30412.
- 6 Su-ping H, Ke-chao Z, Zhi-you L. Inhibition mechanism of aspartic acid on crystal growth of hydroxyapatite. *Trans Nonferrous Met Soc China* 2007; 17: 612-616.
- 7 Shi D, Nakamura T, Dai J, Yi L, Qin J, Chen D, Xu Z, Wang Y, Ikegawa S, Jiang Q. Association of the aspartic acid-repeat polymorphism in the asporin gene with age at onset of knee osteoarthritis in Han Chinese Population. *J Hum Genet* 2007; 52: 664-667.
- 8 Dobosz IN, Janik P. Amino acids acting as transmitters in amyotrophic lateral sclerosis (ALS). *Acta Neurol Scand* 1999; 100: 6-11.
- 9 Aniello AD, Lee JM, Petrucelli L, Fiore MMD. Regional decreases of free d-aspartate levels in Alzheimer's disease. *Neurosci Lett* 1998; 250: 131-134.
- 10 Gashti MP, Bourquin M, Stir M, Hulliger J. Glutamic acid inducing kidney stone biomimicry by a brushite/gelatin composite. *J Mater Chem B* 2013; 1: 1501-1508.
- 11 Dhakal R, Bajpai VK, Baek KH. Production of gaba (γ – Aminobutyric acid) by microorganisms: a review. *Braz J Microbiol* 2012; 4: 1230-1241.
- 12 Hassel B, Dingledine R. *Basic Neurochemistry (Eighth Edition) Principles of Molecular, Cellular, and Medical Neurobiology* 2012; 342-366.
- 13 Chapman J, and Zhou M. Microplate-based fluorometric methods for the enzymatic determination of l-glutamate: application in measuring l-glutamate in food samples. *Analytica Chimica Acta* 1999; 402: 47-52.
- 14 Obayashi Y, Nagamura Y. Does monosodium glutamate really cause headache? : a systematic review of human studies. *J Headache Pain* 2016; 17: 54.
- 15 Dávalos A, Castillo J, Serena J, Noya M. Duration of glutamate release after acute ischemic stroke. *Stroke* 1997; 28: 708-710.
- 16 Hubbard JA, Binder DK. *Astrocytes and Epilepsy: Glutamate Metabolism*. Academic Press 2016, p197-224.

- 17 Boucher JL, Charret C, Coudray-Lucas C, Giboudeau J, Cynober L. Amino acid determination in biological fluids by automated ion-exchange chromatography: performance of Hitachi L-8500A. *Clin Chem* 1997; 43: 1421-1428.
- 18 Mayadunne R, Nguyen TT, Marriott PJ. Amino acid analysis by using comprehensive two-dimensional gas chromatography. *Anal Bioanal Chem* 2005; 3: 836–847.
- 19 Dettmer K, Stevens AP, Fagerer SR, Kaspar H, Oefner, PJ. Amino acid analysis in physiological samples by GC-MS with propyl chloroformate derivatization and iTRAQ-LC-MS/MS. *Methods Mol Biol* 2012; 828: 165-81.
- 20 Vardanega D, Girardet C. Nonlinear polarization effects in superchiral nanotube sensors of amino acids. *Chem Phys Lett* 2009; 469: 172-176.
- 21 Kitagawa F, Otsuka K. Recent progress in capillary electrophoretic analysis of amino acid enantiomers. *J Chromatogr B* 2011; 879: 3078-3095.
- 22 Zhou Y, Nagaoka T, Yu B, Levon K. Chiral Ligand Exchange Potentiometric Aspartic Acid Sensors with Polysiloxane Films Containing a Chiral Ligand N-Carbobenzoxy-Aspartic Acid. *Anal Chem* 2009; 81: 1888–1892.
- 23 Snoek LC, Kroemer RT, Hockridge MR and Simons JP. Conformational landscapes of aromatic amino acids in the gas phase: Infrared and ultraviolet ion dip spectroscopy of tryptophan. *PhysChemChemPhys* 2001; 3: 1819-1826.
- 24 Wang L, He X, Guo Y, Xu J, Shao S. pH-Responsive chromogenic-sensing molecule based on bis(indolyl)methene for the highly selective recognition of aspartate and glutamate. *Beilstein J Org Chem* 2011; 7: 218–221.
- 25 Zhou X, Yip YW, Chan WH, Lee AWM. An easy assembled fluorescent sensor for dicarboxylates and acidic amino acids. *Beilstein J Org Chem* 2011; 7: 75–81.
- 26 Huang XH, He YB, Chen ZH, Hu CG, Qing GY. Novel chiral fluorescent chemosensors for malate and acidic amino acids based on two-arm thiourea and amide. *Can J Chem* 2008; 86: 170-176.
- 27 Kwong HL, Wong WL, Lee CS, Yeung CT, Teng PF. Zinc(II) complex of terpyridine-crown macrocycle: A new motif in fluorescence sensing of zwitterionic amino acids. *Inorg Chem Commun* 2009; 12: 815–818.
- 28 Leung D, Andersen JFF, Lynch VM, and Anslyn EV. Using Enantioselective Indicator Displacement Assays To Determine the Enantiomeric Excess of α -Amino Acids. *J Am Chem Soc* 2008; 130: 12318–12327.
- 29 Andersen JFF, Lynch VM, Anslyn EV. Colorimetric Enantiodiscrimination of α -Amino Acids in Protic Media. *J Am Chem Soc* 2005; 127: 7986-7987.

- 30 Aït-Haddou H, Wiskur S. L, Lynch VM, Anslyn EV. Achieving Large Color Changes in Response to the Presence of Amino Acids: A Molecular Sensing Ensemble with Selectivity for Aspartate. *J Am Chem Soc* 2001; 123: 11296-11297.
- 31 Chinta JP, Acharya A, Kumar A, Rao CP, Spectroscopy and Microscopy Studies of the Recognition of Amino Acids and Aggregation of Proteins by Zn(II) Complex of Lower Rim Naphthylidene Conjugate of Calix[4]arene. *J Phy Chem B* 2009; 113: 12075–12083.
- 32 Zhao X, Wei R, Chen L, Jina D, Yan X. Glucosamine modified near-infrared cyanine as a sensitive colorimetric fluorescent chemosensor for aspartic and glutamic acid and its applications. *New J Chem* 2014; 38: 4791-4798.
- 33 Weng H, Yan B. A silver ion fabricated lanthanide complex as a luminescent sensor for aspartic acid. *Sens Actuator B-Chem* 2017; 253: 1006–1011.
- 34 Lin WC, Tseng YP, Lin CY, Yen YP. Synthesis of alanine-based colorimetric sensors and enantioselective recognition of aspartate and malate anions. *Org Biomol Chem* 2011; 9: 5547-5553.
- 35 Xu M, Huo F, Yin C. A supramolecular sensor system to detect amino acids with different carboxyl groups. *Sens Actuator B-Chem* 2017; 240: 1245–1250.
- 36 Nasomphan W, Tangboriboonrat P, Tanapongpipat S, Smanmoo S. Selective Fluorescent Detection of Aspartic Acid and Glutamic Acid Employing Dansyl Hydrazine Dextran Conjugate. *J Fluoresc* 2014; 24: 7–11.
- 37 Liu SY, Fang L, He YB, Chan WH, Yeung KT, Cheng YK, Yang RH. Cholic-Acid-Based Fluorescent Sensor for Dicarboxylates and Acidic Amino Acids in Aqueous Solutions. *Org Lett* 2005; 26: 5825-5828.
- 38 Hussain MM, Rahman MM, Asiri AM, Rabiul Awual Md. Non-enzymatic simultaneous detection of L-glutamic acid and uric acid using mesoporous Co_3O_4 nanosheets. *RSC Adv* 2016; 6: 80511-80521.
- 39 Guan H, Zhou P, Zhou X, He Z. Sensitive and selective detection of aspartic acid and glutamic acid based on polythiophene-gold nanoparticles composite. *Talanta* 2008; 77: 319–324.
- 40 Bonizzoni M, Fabbrizzi L, Piovani G, Taglietti A. Fluorescent detection of glutamate with a dicopper(II) polyamine cage. *Tetrahedron* 2004; 60: 11159–11162.
- 41 Zhou Y, Yoon J. Recent progress in fluorescent and colorimetric chemosensors for detection of amino acids. *Chem Soc Rev* 2012; 41: 52–67.
- 42 Yin C, Huo F, Cooley NP, Spencer D, Bartholomew K, Barnes CL, Glass TE. A Two-Input Fluorescent Logic Gate for Glutamate and Zinc. *ACS Chem Neurosci* 2017; 6: 1159–1162.
- 43 Buryak A, Severin K. A Chemosensor Array for the Colorimetric Identification of 20 Natural Amino Acids. *J Am Chem Soc* 2005; 127: 3700–3701.

- 44 Joyce LA, Maynor MS, Dragna JM, Cruz GM, Lynch VM, Canary JW, Anslyn EV. A Simple Method for the Determination of Enantiomeric Excess and Identity of Chiral Carboxylic Acids. *J Am Chem Soc* 2011; 133: 13746–13752.
- 45 Boens N, Leen V, Dehaen W. Fluorescent indicators based on BODIPY. *Chem Soc Rev* 2012; 41: 1130–1172.
- 46 Wang F, Zhou L, Zhao C, Wang R, Fei Q, Luo S, Guo Z, Tian H, Zhu W.H. A dual-response BODIPY-based fluorescent probe for the discrimination of glutathione from cysteine and homocysteine. *Chem Sci* 2015; 6: 2584–2589.
- 47 Niu LY, Guan YS, Chen YZ, Wu LZ, Tung CH, Yang QZ. BODIPY-Based Ratiometric Fluorescent Sensor for Highly Selective Detection of Glutathione over Cysteine and Homocysteine. *J Am Chem Soc* 2012, 134, 18928–18931.
- 48 Jia MY, Niu LY, Zhang Y, Yang QZ, Tung CH, Guan YF, Feng L. BODIPY-Based Fluorometric Sensor for the Simultaneous Determination of Cys, Hcy, and GSH in Human Serum. *ACS Appl Mater Interfaces* 2015, 7, 5907–5914.
- 49 Adhikari S, Ghosh A, Mandal S, Guria S, Banerjee PP, Chatterjee A, Das D. Colorimetric and fluorescence probe for the detection of nano-molar lysine in aqueous medium. *Org Biomol Chem* 2016; 14: 10688–10694.
- 50 Jiang XD, Yue S, Jia L, Li S, Li C, Li Q, Xiao L. NIR Fluorescent AzaBODIPY-Based Probe for the Specific Detection of L-Lysine. *Chemistry Select* 2018; 3: 7581 – 7585.
- 51 Munusamy SK, Thirumorthy K, Muralidharan VP, Balijapalli U, Iyer SK. Enantioselective fluorescent sensing of chiral carboxylic acid by engaging boronic acid and BINOL. *Sens Actuator B-Chem* 2017; 244: 175–181.
- 52 Goswami S, Hazra A, Chakrabarty R, Fun HK. Recognition of Carboxylate Anions and Carboxylic Acids by Selenium-Based New Chromogenic Fluorescent Sensor: A Remarkable Fluorescence Enhancement of Hindered Carboxylates. *Org Lett* 2009; 11: 4350–4353.
- 53 Kusukawa T, Tessema EA, Hoshihara Y. A Turn-on Fluorescence Sensor for Dicarboxylic Acids Based on Aggregation-induced Emission. *Chem. Lett* 2018; 47: 1395–1398.
- 54 Benesi HA, Hildebrand JH. A Spectrophotometric Investigation of the Interaction of Iodine with Aromatic Hydrocarbons. *J Am Chem Soc* 1949; 71: 2703.
- 55 M. J. Frisch, G. W. Trucks, H. B. Schlegel, G. E. Scuseria, M.A. Robb, J. R. Cheeseman, et al. *Gaussian 09*, revision A.02. Wallingford, CT: Gaussian, Inc. 2009.

Highlights

1. A highly selective BODIPY probe, N,N-SP-BPY detects aspartic acid (Asp) and glutamic acid (Glu) in water.
2. 'Turn On' fluorescence can be observed by inhibition of Photoinduced Electron Transfer (PET) process.
3. A distinct colorimetric change from pink to colourless solution can be observed to recognize Asp and Glu.
4. N,N-SP-BPY efficiently images intracellular Asp and Glu in live cells under fluorescence microscope.